MAGNETIC RESONANCE IN CHEMISTRY, VOL. 36, 285–295 (1998)

Conformation of Renin Substrate (Angiotensinogen) in Water is Different from DMSO: a ^{1}H NMR and Molecular Dynamics Study

Anant B. Patel,[1] Sudha Srivastava,[1]* Ratna S. Phadke,[1] Evans Coutinho[2] and Shantaram Kamath[2]

[1] Chemical Physics Group, Tata Institute of Fundamental Research, Homi Bhabha Road, Colaba, Mumbai 400 005, India
[2] Bombay College of Pharmacy, Kalina, Mumbai 400 098, India

Received 9 July 1997; revised 26 September 1997; accepted 1 October 1997

ABSTRACT: The conformation of angiotensinogen, a tetradecapeptide, with the sequence Asp1–Arg2–Val3–Tyr4–Ile5–His6–Pro7–Phe8–His9–Leu10–Leu11–Val12–Tyr13–Ser14, was studied in aqueous medium by 2D NMR spectroscopy. Complete resonance assignments were made using a combination of DQF-COSY, TOCSY and NOESY spectra. The kinetics of deuterium exchange of NH protons were also studied. The NMR results indicate the presence of at least two conformations in dynamic equilibrium. A total of 39 NOEs were used in the restrained molecular dynamics simulation to generate the solution structure. The dominant conformation of angiotensinogen is characterized by a β-turn around the tetrapeptide sequence Val3–Tyr4–Ile5–His6, two γ-bends at Tyr4 and Leu10 and a sharp turn around Val12. The conformation of angiotensinogen in water is radically different from the conformation in DMSO reported earlier.

KEYWORDS: NMR; ^{1}H NMR; angiotensinogen; conformation; deuterium exchange; restrained molecular dynamics

INTRODUCTION

The renin–angiotensin system (RAS) is composed of renin (an endopeptidase), angiotensinogen (a tetradecapeptide with sequence D–R–V–Y–I–H–P–F–H–L–L–V–Y–S) and angiotensin-converting enzyme (ACE, a zinc metalloproteinase). The RAS plays a vital role in the body in the control of blood pressure. Hence any malfunction in this system appears to be an important contributing factor in hypertensive diseases.[1]

Renin cleaves angiotensinogen between the two leucine residues Leu10–Leu11 to liberate the decapeptide angiotensin I.[1] At the endothelial surface of blood vessels in the lungs and other tissues, angiotensin I is broken down to the octapeptide angiotensin II by ACE.[2] Angiotensin II is a powerful vasoconstrictor. Finally, angiotensinase A cleaves angiotensin II to the heptapeptide angiotensin III, which is about 50% as potent as angiotensin II.[3] The rate-limiting step in this cascade of reactions is the cleavage of the Leu10–Leu11 bond, which is catalyzed by renin.[4] Therefore, inhibition of this step would have substantial value in the management of hypertension. A thorough understanding of the 3D structure and dynamics of angiotensinogen will therefore have great potential in the design of suitable and effective renin inhibitors.

We reported earlier the conformation of angiotensinogen in DMSO by NMR and MD simulations.[5] In this paper we report our investigations of the conformation of angiotensinogen in water by 2D NMR spectroscopy and restrained molecular dynamics (MD) simulations.

* *Correspondence to*: S. Srivastava, Chemical Physics Group, Tata Institute of Fundamental Research, Homi Bhabha Road, Colaba, Mumbai 400 05, India
E-mail: sudha@tifrvax.tifr.res.in

EXPERIMENTAL

Angiotensinogen was purchased from Sigma (St Louis, MO, USA) and used without further purification. Its purity was checked by ^{1}H NMR spectroscopy.

NMR experiments

Samples for NMR experiments were prepared by dissolving 10 mg of the peptide in 0.6 ml of H_2O–D_2O (9:1) and adjusting the pH to 4.0. NMR experiments were carried out on a Varian Unity Plus 600 MHz NMR spectrometer. The data were processed on an IRIS Indigo workstation using Felix software (v. 2.30) supplied by MSI (San Diego, CA, USA).

For resonance assignments, DQF-COSY[6] and TOCSY[7] spectra were recorded. NOESY spectra[8] were recorded with mixing times of 50, 100, 200 and 300 ms. The water resonance was suppressed by presaturation during the relaxation period (1 s). All the spectra were recorded using the hypercomplex (STATES) method[9] with the conventional pulse sequences, an 8000 Hz spectral width, 512 and 2048 data points in the t_1 and t_2 dimensions, respectively, and 32 scans per t_1 increment. Gradient enhanced HSQC spectra were recorded using the standard pulse sequence.[10] The parameters used were relaxation delay 1.5 s and spectral width for the

CCC 0749-1581/98/040285–11 $17.50

^{1}H and ^{13}C dimensions 7000 and 13 000 Hz with 2048 and 512 data points, respectively. The data were apodized by a shifted sine-bell window function and zero filled to a 2D matrix of size 4K × 2K prior to Fourier transformation.

The kinetics of deuterium exchange were measured in the following manner. The peptide was dissolved in 100% D_2O and a 1D spectrum was recorded at regular time intervals up to 70 min. In each case, 32 scans were accumulated. The middle of the duration of each experiment was taken as the time for the corresponding data. The integrated intensity (I) of each NH resonance was observed to decrease exponentially with time (t) as $I_{(t)} = I_{(0)} \exp(-kt)$, where k is the exchange rate constant, $I_{(t)}$ is the intensity at time t and $I_{(0)}$ that at $t = 0$. The exchange rates were obtained from a least-squares analysis of the semi-logarithmic plots of signal intensities as a function of time. In cases where two NH protons overlap, the data could only be fitted to a double exponential equation: $I_{(t)} = I_{(1)} \exp(-k_1 t) + I_{(2)} \exp(-k_2 t)$ with two corresponding exchange rate constants k_1 and k_2, owing to the different exchange rates.

The NOESY spectrum recorded with a mixing time of 100 ms was integrated. The peak volumes were converted into distances using the inverse sixth power relationship of intensity with distance.[11] The NOE between the H-2 and H-4 protons of His6, which are 4.78 Å apart, was selected as the reference for intensity to distance conversion.

Molecular dynamics simulations

Calculations were performed on a Silicon Graphics IRIS Indigo workstation with MSI software (Insight II v. 2.3 and Discover v. 2.9). Using the Biopolymer module, a fully extended peptide with the side-chains of Asp1, Arg2, His6 and His9 and the N and C termini ionized was constructed to match the NMR study. The molecule was then centered in a box (of dimensions 45 × 25 × 25 Å) and soaked with 813 water molecules with the SOAK program. The energy of the system was calculated with the CFF91 forcefield.[12] The bond stretching was described by a harmonic approximation. No cross-terms were included in the energy expression. The dielectric constant was fixed as 1.0. A cut-off of 14 Å was used for the non-bonded energy evaluation.

Molecular dynamics calculations were performed with the following protocol. The energy of the system was minimized first with 500 steps of steepest descent, followed by 1000 steps of conjugate gradients to relax the waters and to remove any strain in the starting conformation of the peptide. A forcing potential of 30 kcal mol^{-1} rad^{-2} was applied to all omega angles to keep them in the *trans* configuration during the simulation. A total of 39 observed NOEs were used as distance restraints by incorporation of an additional harmonic term $K(R_{ij} - R_{\text{target}})^2$ to the forcefield. The force constant K was set to 50.0 kcal mol^{-1} Å^{-2} when R_{ij} varied both greater than or less than R_{target} (soft forces). The maximum force that was allowed to be applied to satisfy the constraint was 1000 kcal mol^{-1}. The distance between the constrained protons (R_{target}) was set to ±0.2 Å (upper and lower bounds) from the calculated distances (see above).

Newton's equations of motion were integrated with the Verlet algorithm[13] with an integration time step of 1 fs. The system was equilibrated at 300 K for 20 ps. Dynamics were continued for another 50 ps. The structures for the MD trajectory were sampled every 1 ps and stored to generate 50 structures. Temperature control during equilibration was achieved by direct velocity scaling, whereas during the data collection period (50 ps) a weak coupling to the temperature bath with a coupling constant of 0.1 ps was used. At the end of the MD run all 50 structures were energy minimized, beginning with steepest descent followed by a conjugate gradient until the derivative of energy fell below 0.01 kcal mol^{-1} Å^{-1}.

RESULTS AND DISCUSSION

Resonance assignments

The 1D NMR spectrum of angiotensinogen in water is shown in Fig. 1. Identification of the spin systems and assignments of individual resonances were made from DQF-COSY and TOCSY spectra. In the fingerprint region of the DQF-COSY spectrum (Fig. 2) there are more cross peaks than expected. This indicates that more than one conformation exists simultaneously. The spin systems of the amino acids in angiotensinogen can be broadly classified into the following five groups: Asp, Tyr, His, Phe, Ser [AMX]; Arg, Pro [$A_2(T_2)$MPX]; Val[A_3B_3MX]; Ile [A_3MPT(B_3)X]; and Leu [A_3B_3MPTX]. From the NH resonances in the TOCSY spectrum (Fig. 3), the spin systems were identified and the different amino acids grouped together. It is possible to identify Ser14 uniquely since its CβH protons occur more downfield than the others in that group.

For sequence-specific assignments, the fingerprint region of the NOESY spectrum was used (Fig. 4). We start with the NH–CαH COSY peak of Ser14. A vertical line joins the NOESY cross peak to Tyr13. A horizontal line leads to the COSY cross peak to Tyr13. Again moving up, we find the NOESY cross peak to the previous residue Val12. Continuing in this fashion all peaks upto Pro7 could be assigned. Because of the absence of an NH proton in Pro7, a break occurs in the sequential assignment. This break could be joined by an NOE observed between the CδH of Pro7 and CαH of His6. This NOE also fixes the His6–Pro7 bond in the *trans* configuration. Having identified the CαH of His6, the remaining resonances could be assigned by walking vertically and horizontally through COSY–NOESY peaks as described above.

The extra cross peaks (weak intensity) in the fingerprint region of the COSY spectrum were assigned as Val3′, Tyr4′, Ile5′ and His6′ based on the number and

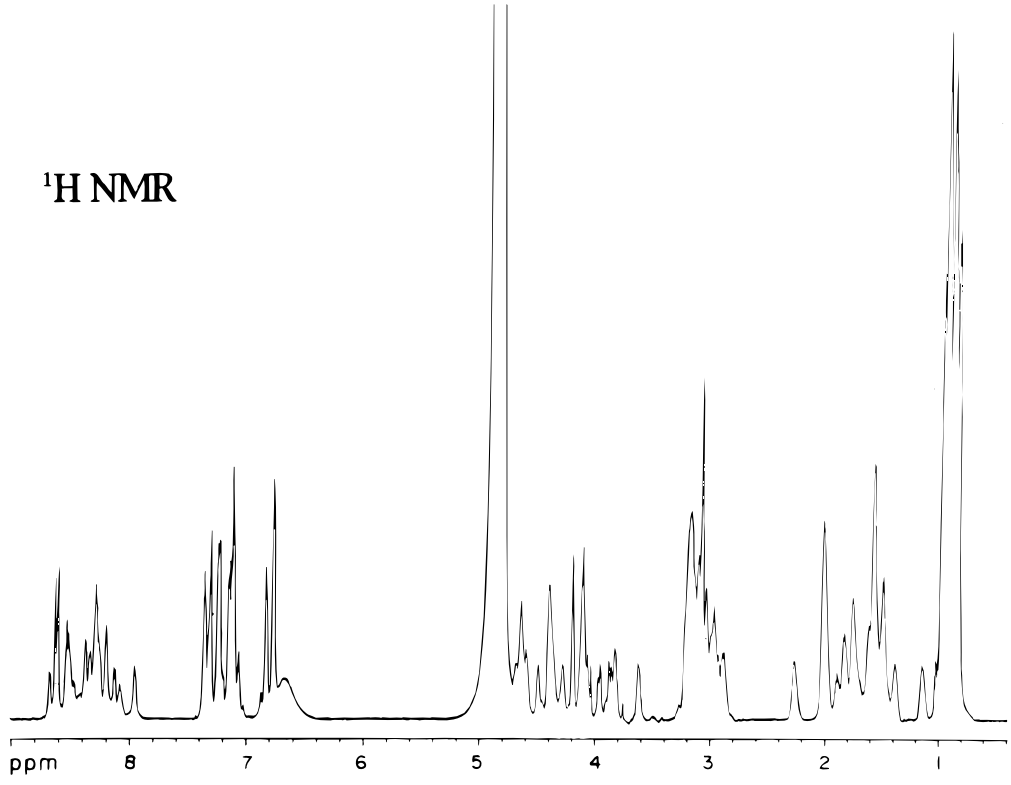

Figure 1. 600 MHz ^{1}H NMR of angiotensinogen in water at pH $\approx$ 4.0 and 298 K.

position of cross peaks to be expected for such spin systems. The prime denotes that these resonances result from a second minor conformation of angiotensinogen. The remaining resonances (Asp1, Arg2, Pro7, Phe8, His9, Leu10, Leu11, Val12, Tyr13 and Ser14) overlap with the respective resonances of the first conformation. An interesting feature of this second conformation is that the His6–Pro7 bond is *cis*, as is evident from the presence of a cross peak between the CαH resonances of these amino acids. Hence the second conformation of the molecule has a different structure around the pentapeptide segment Val–Tyr–Ile–His–Pro. The chemical shifts of all resonances in the two conformations are given in Table 1. Chemical shifts are referenced to the ^{1}H resonance of water at 4.78 ppm.

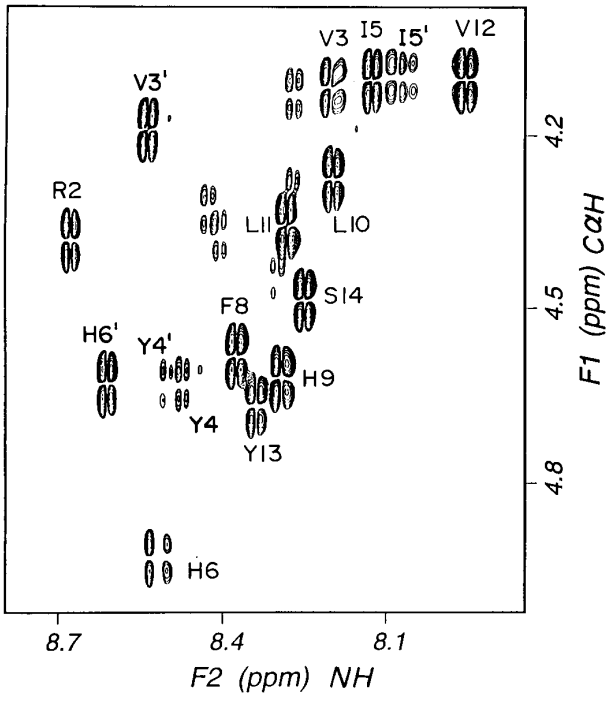

Figure 2. 600 MHz DQF-COSY spectrum of angiotensinogen in H_2O–D_2O (9:1) at 298 K and pH $\approx$ 4.0 indicating the NH to CαH correlations. F_1 = 4.2–4.8 ppm; F_2 = 7.7–8.8 ppm. Peaks are labeled with single-letter codes for amino acids.

Conformation

NH exchange rate. Owing to overlap of resonances in the NH region, it was difficult to measure accurately the temperature coefficient of NH chemical shifts from 1D spectra recorded at different temperatures. Information on hydrogen bond or solvent shielding was therefore obtained by measuring the kinetics of deuterium exchange of NH protons.[14–16] A semi-logarithmic plot of NH resonance intensity against time (Fig. 5) shows that the exchange of these NH protons obeys pseudo-first order kinetics, i.e. the signal intensity decreases exponentially with time. Rate constants calculated from the least-squares analysis of signal intensities as a function of time are given in Table 2. It is evident that the exchange rate constants increase in the order VAl12 < Tyr13 < His6 < Tyr4, whereas the order for those for overlapping residues is His9/Leu11 < Val3/Leu10. For these, the exchange rate constant could not be unambiguously assigned to the individual residues.

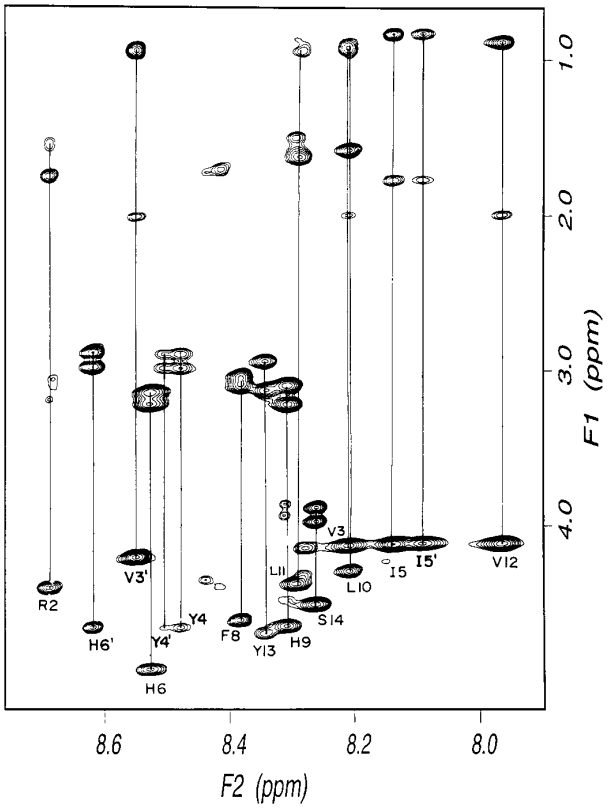

Figure 3. 600 MHz TOCSY spectrum of angiotensinogen in H_2O–D_2O (9 : 1) at 298 K and pH $\approx$ 4.0 indicating the spin system of the amino acids. The NH-CαH cross peaks are labeled with single-letter codes for amino acids.

The large difference in the NH exchange rate suggests that some of these NH protons are either involved in H-bonding or are sequestered from the solvent.

^{13}C chemical shifts. Figure 6 shows ^{13}Cα region of the HSQC spectrum of the peptide at 298 K. ^{13}Cα chemical shifts of all the carbons are listed in Table 3. It is observed that these values depart from the chemical shift values reported for the random coil structure.[17,18] The possible effect of these changes in ^{13}Cα chemical shifts on the conformation have been well discussed in case of proteins and peptides.[18,19] Our results indicate the existence of a rigid structure in angiotensinogen.

^3J(NHCαH) values. The ^3J(NHCαH) values, which are large ($\geq$ 7.5 Hz), indicate that the major conformation must be in dynamic equilibrium with the second conformation that has a more or less extended backbone arrangement. The backbone (ϕ, ψ) and side-chain (χ_1, χ_2, etc.) torsion angles in this conformation are listed in Table 4.

NOE data. A large number of both intra- and inter-residue NOEs are seen for angiotensionogen in water (Fig. 7). A survey of all the observed NOEs is given in Fig. 8. Some important long range NOEs are between CαH of Leu10 and NH of Tyr13 ($\alpha_i \rightarrow NH_{i+3}$); Val3 C$\alpha$H to His6 NH ($\alpha_i \rightarrow NH_{i+3}$); Ile5 C$\alpha$H to Phe8 NH ($\alpha_i \rightarrow NH_{i+3}$); and C$\alpha$H of His9 to C$\alpha$H of Val12

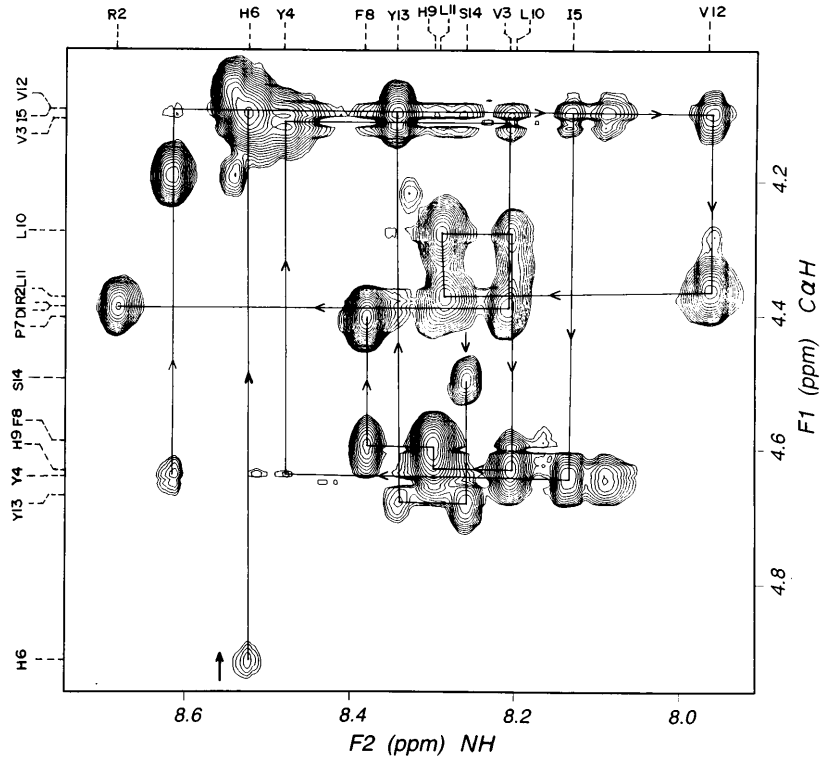

Figure 4. NH–CαH region (F_1 = 4.2–5.0 ppm; F_2 = 7.8–8.8 ppm) of the 600 MHz NOESY spectrum of angiotensinogen recorded with a 200 ms mixing time in H_2O–D_2O (9 : 1) at 298 K and pH $\approx$ 4.0 showing the sequential assignments.

Table 1. Chemical shifts of different protons of angiotensinogen in water at pH ≈4.0 and 298 K

	Chemical shift (ppm)			
Amino acid	NH	CαH	CβH	CγH and other
Asp1	—	4.40	3.05, 2.99	—
Arg2	8.69	4.40	1.76	1.50; δCH_2 3.14, NH, 7.06
Val3	8.21	4.12	2.00	0.91
Val3′	8.55	4.20	2.02	0.93
Tyr4	8.48	4.67	2.90, 2.99	H(2,6) 7.12; H(3,5) 6.78
Tyr4′	8.51	4.65	2.90, 2.99	H(2,6) 7.12; H(3,5) 6.78
Ile5	8.11	4.12	1.78	γCH_2 1.40, 1.17; γCH_3 0.85; δCH_3 0.86
Ile5′	8.09	4.12	1.78	γCH_2 1.40, 1.17; γCH_3 0.85; δCH_3 0.86
His6	8.52	4.96	3.22, 3.15	H2 8.63; H4 7.24
His6′	8.63	4.66	2.89, 2.99	H2 8.63; H4 7.24
Pro7	—	4.42	1.84, 2.28	2.03, δCH_2 3.65, 3.85
Phe8	8.38	4.61	3.06	H(2,6), 7.26; H(3,5) 7.37; H4 7.31
His9	8.31	4.65	3.11, 3.22	H2 8.65; H4 7.32
Leu10	8.21	4.29	1.59	0.96
Leu11	8.29	4.38	1.63	0.93
Val12	7.96	4.12	2.00	0.89
Tyr13	8.34	4.69	2.94. 3.14	H(2,6) 7.16; H(3,5) 6.84
Ser14	8.26	4.51	3.89, 3.98	—

($\alpha_i \rightarrow \alpha_{i+3}$). These NOEs along with the NH exchange rates indicate that angiotensinogen is well structured with only the *C*- and *N*-terminal ends being poorly defined.

Restrained molecular dynamics

The 50 structures obtained by restrained MD simulation were analyzed. Before discussing the simulated structures we shall consider briefly the NOEs used as distance restraints in the MD simulation. From the preceding discussion it is clear that at least two different conformations exist for angiotensinogen whose resonances overlap, except for Val3, Tyr4, Ile5 and His6. Thus, most of the measured NOEs will be a sum of the intensities arising from these two different conformations. These NOEs are used to simulate a single structure by MD calculations. Therefore, *a priori* it is very unlikely that the full set of 39 distance restraints would

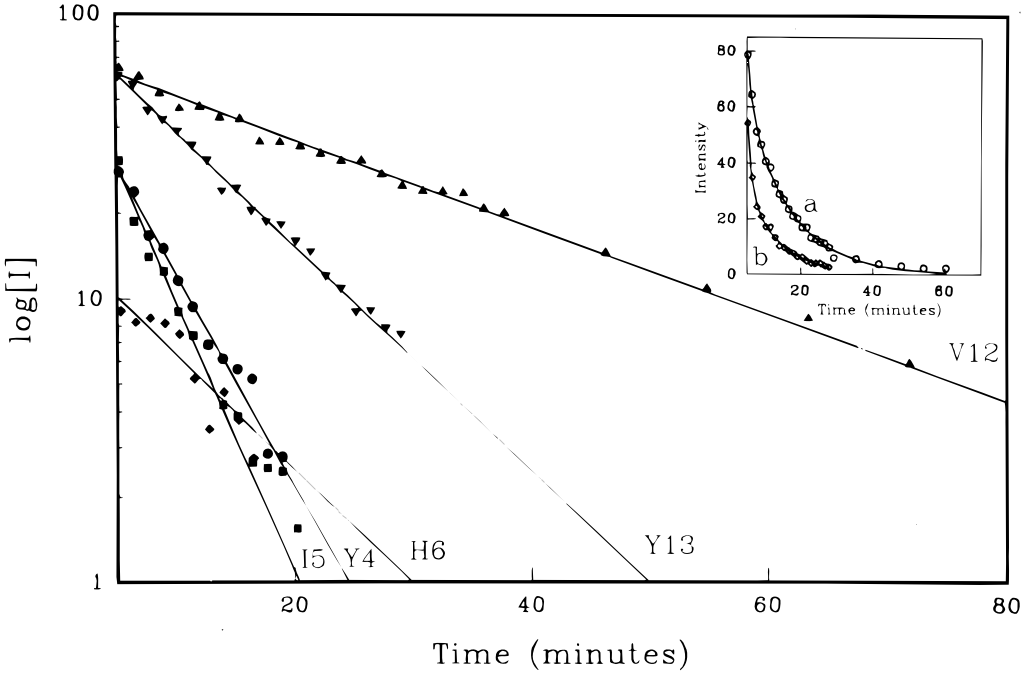

Figure 5. Semi-logarithmic plot of NH resonance intensities with time. The points represent the experimental values; the lines are drawn by exponential fitting. The inset is the plot of signal intensity against time for the residues V3/L10 and H9/L11. The points are experimental values and the lines are drawn by double exponential fitting to these points.

Table 2. Deuterium exchange rate constants of NH protons of angiotensinogen[a]

Residue	Exchange rate constant (10^{-3} s^{-1})
Val3/Leu10	14.2 ± 1.7/1.8 ± 0.1
Tyr4	2.9 ± 0.2
Ile5	3.7 ± 0.3
His6	1.6 ± 0.3
His9/Leu11	10.1 ± 2.4/1.4 ± 0.1
Val12	0.8 ± 0.02
Tyr13	1.6 ± 0.03

[a] For the residues not listed, their NH protons exchange too fast for the exchange rate to be measured.

be fully satisfied in these structures within the limits set in the calculations. The largest distance violations were seen for the proton pairs Leu10 CαH–Tyr13 NH (2.0 Å) and His9 NH–Tyr13 CδH (1.7 Å). For a few pairs the violations in the distances ranged from a low of 0.1 Å to a maximum of 1.7 Å and were fully satisfied in the remaining.

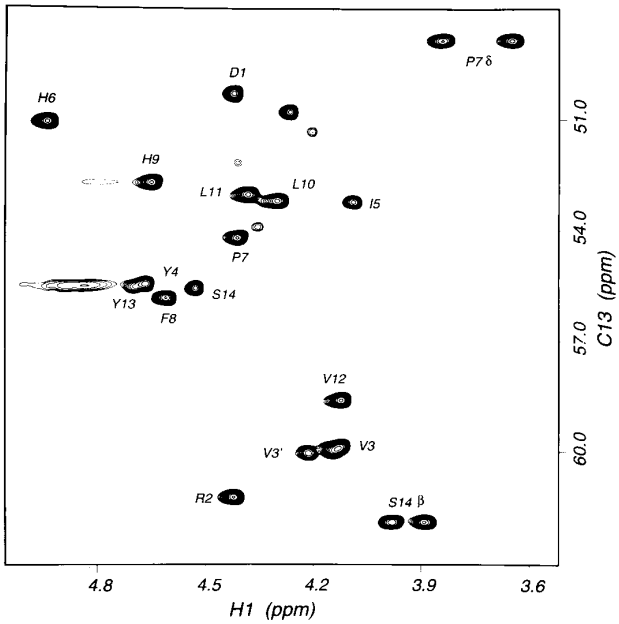

Figure 6. α-Region of sensitivity enhanced HSQC spectrum of angiotensinogen in water at 298 K. Peaks are labeled with single-letter codes for amino acids.

Table 3. $^{13}C\alpha$ chemical shifts of angiotensinogen in water and for amino acids in random coil structure[17,18] in water at 298 K

Residue	In water	A[a]	B[a]
Asp1	50.3	54.2	53.4
Arg2	61.3	56.0	55.0
Val3	59.9	62.2	61.4
Tyr4	55.5	57.9	55.6
Ile5	53.3	61.1	—
His6	51.07	55.0	54.5
Pro7	54.20	63.3	61.7
Phe8	55.8	57.7	—
His9	52.7	45.1	54.5
Leu10	53.2	55.1	52.8
Leu11	53.0	55.1	52.8
Val12	58.6	62.2	61.4
Tyr13	55.5	57.9	55.6
Ser14	55.6	58.3	58.1

[a] A, As reported by Wishart *et al.*;[17] B, as reported by Wishart *et al.*[18]

All 50 structures have β-turns around the tetrapeptide segment Val3–Tyr4–Ile5–His6 with an intramolecular H-bond between Val3 CO and His6 NH together with γ-bends at Tyr4 and Leu10. The β-turn cannot be exactly categorized but resembles Type II. However, the facts that the H-bond distances (N···O = 2.8–2.9 Å and N—H···O = 1.9–2.1 Å) and the distances between the Cα atoms of Val3 and His6 range from 4.6 to 4.8 Å strongly support a β-turn conformation[20] around the segment Val3–Tyr4–Ile5–His6. Both the γ-bends around Tyr4 and Leu10 are of the inverse type and have the preceding and succeeding residues in the characteristic H-bond pattern seen for γ-turns, i.e. there is an H-bond between Val3 CO and Ile5 NH and between His9 CO and Leu11 NH. Again, in all structures there is a sharp turn around Val12 which causes the Leu11 CO to H-bond with the NH of Tyr13. The intramolecular H-bonds associated with

Table 4. Coupling constants[a] of angiotensinogen in water at pH ≈4.0 and 298 K

Amino acid	^3J(NHCαH) (Hz)	Amino acid	^3J(NHCαH) (Hz)
Asp1	—	Pro7	—
Arg2	8.5	Phe8	9.4
Val3	10.1	His9	10.4
Val3′	9.1	Leu10	9.4
Tyr4	8.5	Leu11	8.9
Tyr4′	9.9	Val12	9.4
Ile5	8.5	Tyr13	9.8
Ile5′	13.2	Ser14	8.9
His6 (*trans*)	7.7		
His6′ (*cis*)	8.9		

[a] Coupling constants measured from DQF-COSY spectrum.

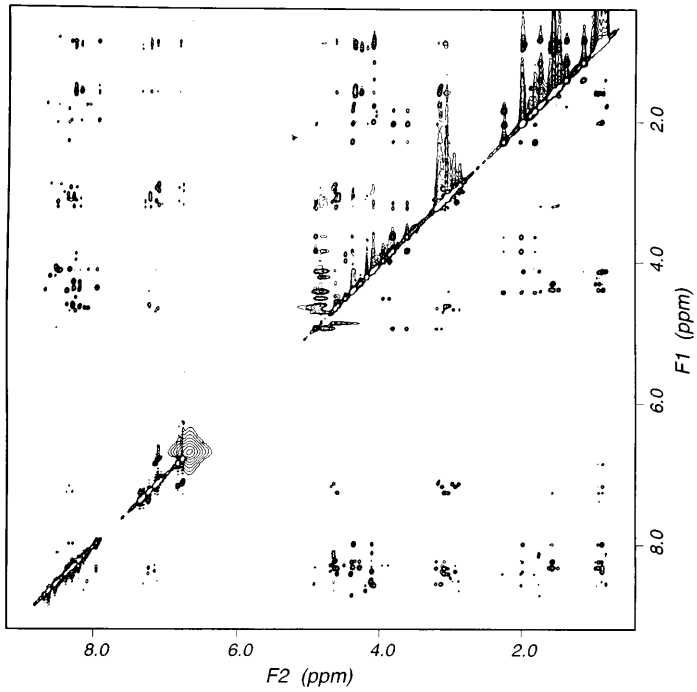

(A)

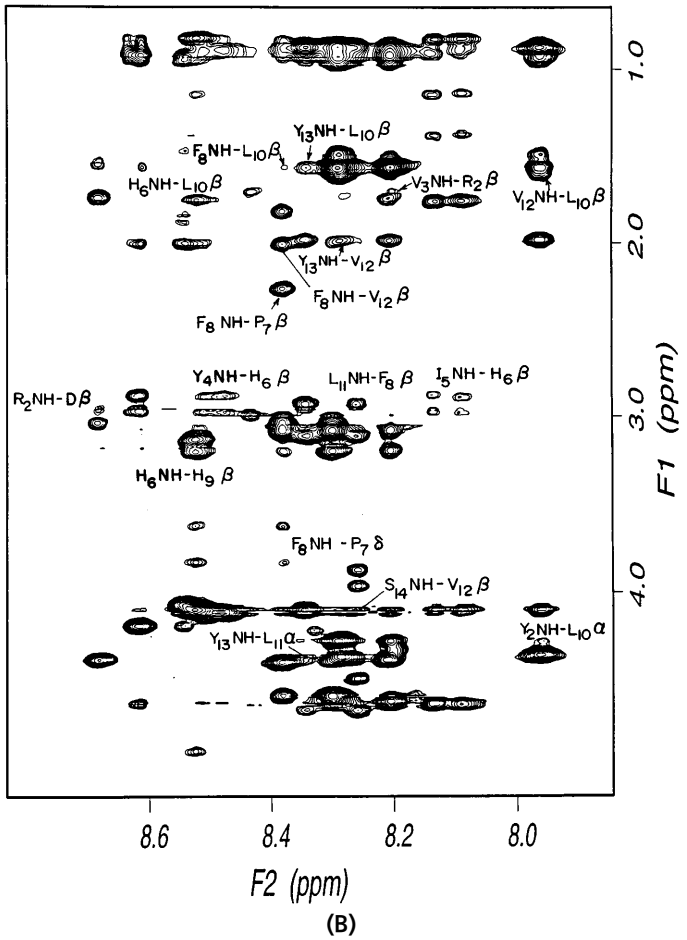

(B)

Figure 7. (A) The full NOESY spectrum of angiotensinogen recorded with a mixing time of 200 ms in H_2O–D_2O (9 : 1) at 298 K and pH $\approx$ 4.0 showing the full range of inter- and intra-residue NOEs. (B) The section (F_1 = 0.7–5.0 ppm, F_2 = 7.8–8.8 ppm) of the NOESY spectrum showing the inter- and intra-residue NOEs. (C) The NH–NH region (F_1 = 7.8–8.9 ppm, F_2 = 7.8–8.9 ppm) of the NOESY spectrum showing the NH–NH cross peaks.

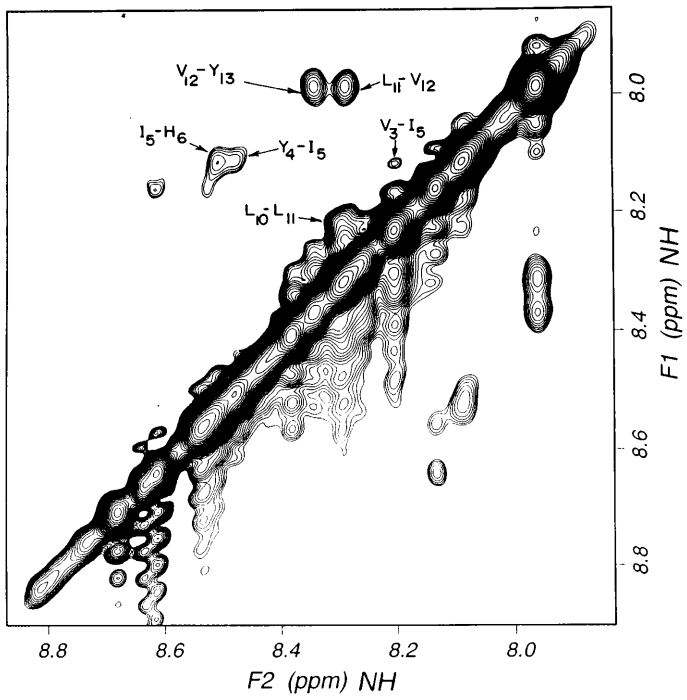

Figure 7. (C)

Figure 8. Schematic diagram of observed NOEs for angiotensinogen.

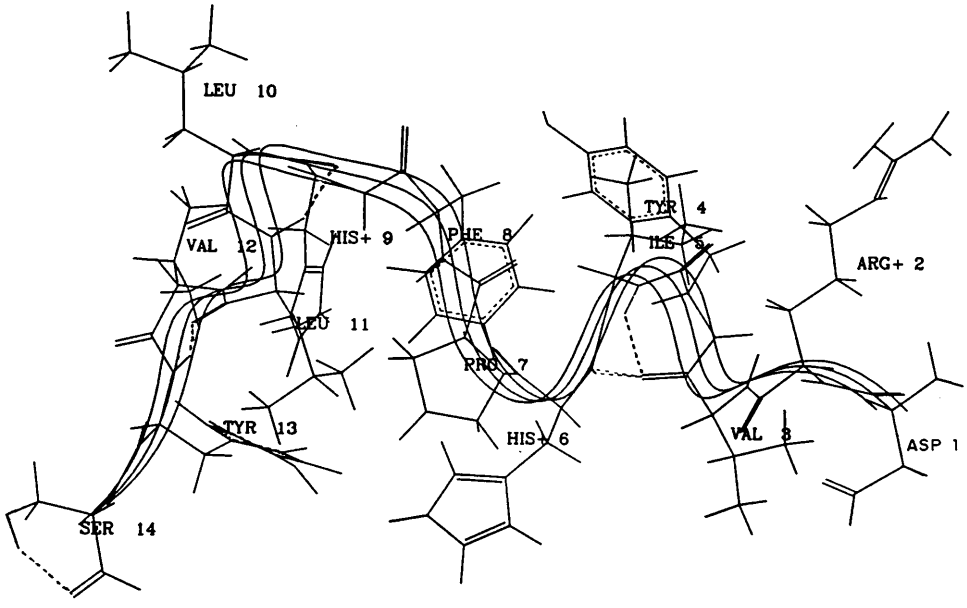

Figure 9. Conformation of angiotensinogen simulated using NOEs as distance restraints. Broken lines indicate H-bonds.

Table 5. Averaged structure and rms deviations for angiotensinogen obtained by restrained MD simulations in water

	Torsion angle[a]						
Residue	ϕ	ψ	χ_1	χ_2	χ_3	χ_4	χ_5
Asp1	—	129 (6)	−176 (6)				
Arg2	−131 (6)	174 (5)	−72 (3)	180 (7)	−179 (6)	−156 (34)	−163 (49)
Val3	−139 (6)	−40 (2)	56 (7)				
Tyr4	−76 (1)	85 (3)	−180 (4)	72 (3)			
Ile5	133 (3)	24 (4)	71 (2)	148 (31)			
His6	−53 (3)	117 (2)	161 (5)	−107 (5)			
Pro7	56 (1)	−146 (4)	−4 (2)	−20 (2)	38 (1)	−40 (1)	
Phe8	124 (5)	29 (2)	−32 (2)	125 (6)			
His9	−39 (1)	−164 (28)	64 (1)	14 (4)			
Leu10	−81 (5)	58 (11)	−76 (12)	176 (4)			
Leu11	22 (7)	74 (1)	159 (1)	−71 (3)			
Val12	−60 (4)	6 (9)	78 (2)				
Tyr13	−119 (10)	160 (5)	−49 (3)	149 (3)			
Ser14	−106 (23)	—	59 (3)				

[a] Average torsion angles in degrees taken over the whole trajectory. Value in parentheses are the rms deviations.

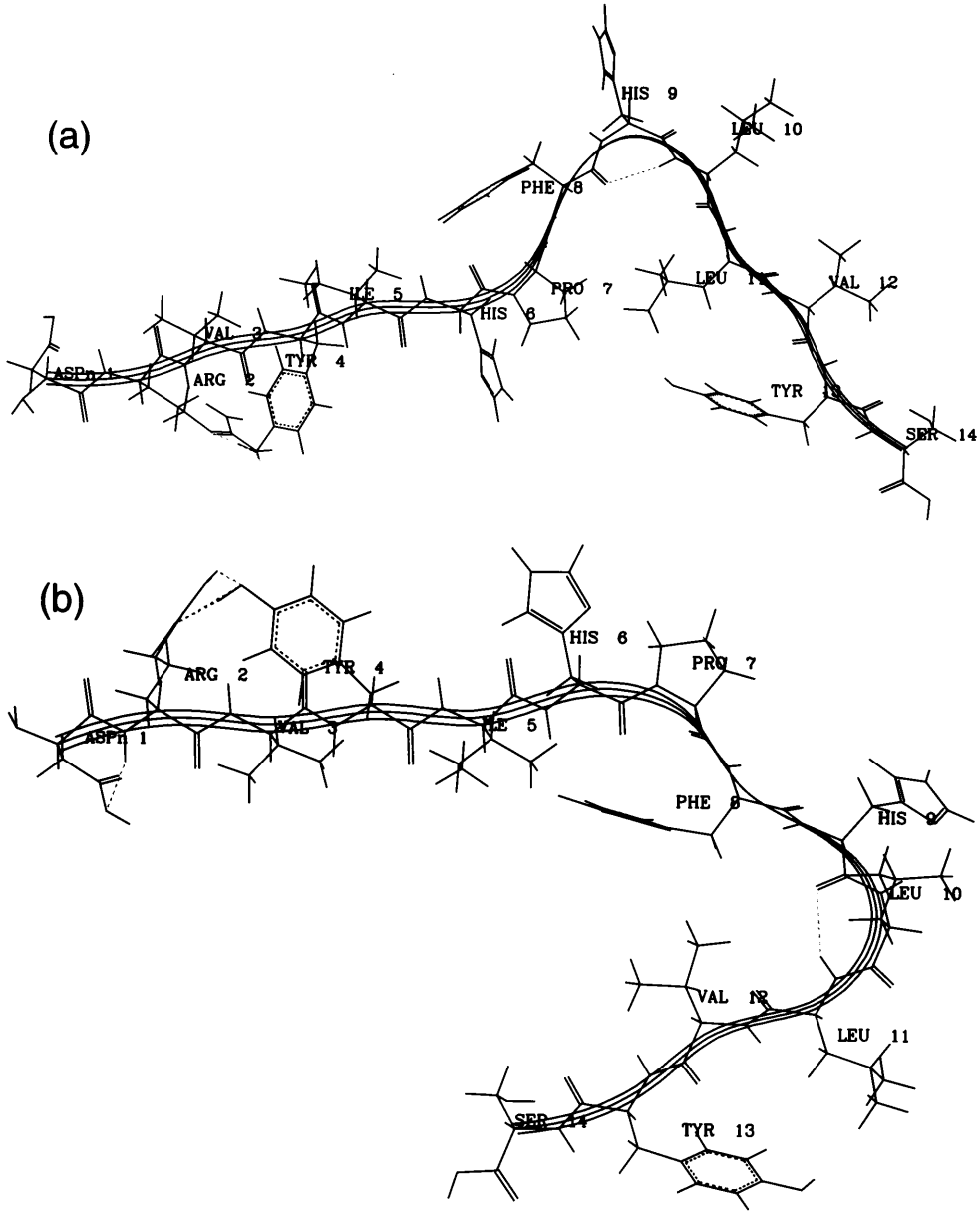

Figure 10. The two conformations of angiotensinogen in DMSO. (a) γ-Bend at His9 and (b) γ-bend at Leu10.

Table 6. Conformational parameters of global minimum of angiotensinogen in water as determined by restrained MD

	Torsion angle (°)						
Residue	ϕ	ψ	χ_1	χ_2	χ_3	χ_4	χ_5
Asp1	—	132	−173				
Arg2	−123	169	−70	169	−173	−118	−167
Val3	−146	−45	39				
Tyr4	−73	90	−179	84			
Ile5	126	28	73	146			
His6	−48	122	165	−96			
Pro7	57	−132	−7	−17	36	−39	
Phe8	111	25	−37	137			
His9	−36	−167	−64	15			
Leu10	−81	65	−70	174			
Leu11	15	74	−161	−76			
Val12	−62	4	79				
Tyr13	−116	165	−53	153			
Ser14	−143	—	61				

secondary structural motifs like the β-turn (Val3–Tyr4–Ile5–His6) and γ-bends (at Tyr4 and Leu10) and also the non-specific bend at Val12 are expected to be reflected in the low deuterium exchange rates for the NH protons of His6, Ile5, Leu11 and Tyr13 (see above). In fact we observed relatively small exchange rate constants for these protons.

Hence the dominant conformation of angiotensinogen in water consists of a β-turn, γ-bends and a non-specific fold. The averaged structure and the rms deviations seen for the whole trajectory are given in Table 5, which shows that there is good homogeneity in the structures generated by MD simulations. As a representative structure, the global minimum of the simulation is drawn in Fig. 9. A second minor conformation also exists which was alluded to earlier. The sparse data available for this conformation make it difficult to assign a definite structure to it. However, it is certain that the His6–Pro7 amide bond is *cis* (see above). Also, in the minor form, the NH resonance of Val3 is close to the value seen in random coil structures, in contrast to its value in the major conformation, but no major change is seen for residues 4–6 (see Table 1).

The two conformations of angiotensinogen in DMSO[5] are depicted in Fig. 10. The common feature in the conformation of angiotensinogen in the two solvents is a γ-bend at Leu10. The differences in the conformation may be a result of solvent polarity and polarizability.

CONCLUSIONS

Angiotensinogen exists in water in at least two different conformations. The major conformation is highly structured with a β-turn around Val3-Tyr4–Ile5–His6, γ-bends at Tyr4 and Leu10 and a non-specific fold around Val12. The other conformation may be more or less extended with a *cis* amide bond between His6 and Pro7. Both conformations are remarkably different from that found in DMSO, where a γ-bend occurs at either His9 or Leu10.[5] The fact that the γ-bend at Leu10 persists even in water strengthens our earlier hypothesis that a γ-bend at Leu10 in angiotensinogen is the recognition element for cleavage by the enzyme renin.

Acknowledgements

The facilities provided by the National Facility for High Field NMR located at TIFR, Mumbai, supported by the Department of Science and Technology (DST), are gratefully acknowledged. The Ministry of Human Resources and Development (MHRD), India, is also thanked for the computational facilities at BCP.

REFERENCES

1. L. T. Skeggs, F. E. Dorer, J. R. Kahn, K. E. Lentz and N. Levine, *Am. J. Med.* **60**, 737 (1976).
2. E. G. Erdös, *Am. J. Med.* **60**, 749 (1976).
3. J. O. Davis and R. R. Freeman, *Biochem. Pharmacol.* **26**, 93 (1977).
4. C. I. Johnston, *Drugs* **39**, 21 (1990).
5. S. Srivastava, R. S. Phadke, E. Coutinho and S. A. Kamath, *Magn. Reson. Chem.* **34**, 651 (1996).
6. U. Piantini, O. W. Sorenson and P. P. Ernst, *J. Am. Chem. Soc.* **104**, 6800 (1982).
7. A. Bax and D. G. Davis, *J. Magn. Reson.* **65**, 355 (1985).
8. A. Kumar, R. R. Ernst and K. Wüthrich, *Biochem. Biophys. Res. Commun.* **95**, 1 (1980).
9. D. J. States, R. A. Habercorn and D. J. Ruben, *J. Magn. Reson.* **48**, 286 (1982).
10. L. E. Kay, P. Keifer and T. Saarinen, *J. Am. Chem. Soc.* **114**, 10663 (1992)
11. R. E. London, M. E. Perlman and D. G. Davis, *J. Magn. Reson.* **97**, 79 (1992).
12. J. Maple, U. Dinur and A. T. Hagler, *Proc. Natl. Acad. Sci. USA* **85**, 5350 (1988).
13. L. Verlet, *Phys. Rev.* **159**, 98 (1967).
14. G. Wagner, C. I. Stassinopoulou and K. Wuthrich, *Eur. J. Biochem.* **145**, 431 (1984).

15. R. Richarz, P. Sehr, G. Wagner and K. Wuthrich, *J. Mol. Biol.* **130**, 19 (1979).
16. D. Hilton and C. W. Woodword, *Biochemistry* **17**, 3325 (1978).
17. D. S. Wishart, C. G. Bigam, A. Holm, R. S. Hodges and B. D. Sykes, *J. Biomol. NMR* **5**, 67 (1995).
18. D. S. Wishart, B. D. Sykes and F. M. Richards, *J. Mol. Biol.* **222**, 311 (1991).
19. M. D. Reily, T. Venkataraman and D. O. Omecinsk, *J. Am. Chem. Soc.*, **114**, 6251 (1992).
20. C. Venkatachalam, *Biopolymers* **6**, 1425 (1968).